TOXICOLOGICAL SCIENCES **72,** 3–18 (2003)
DOI: 10.1093/toxsci/kfg001

Physiological Modeling of Inhalation Kinetics of Octamethylcyclotetrasiloxane in Humans during Rest and Exercise

Micaela B. Reddy,*[,1] Melvin E. Andersen,* Paul E. Morrow,† Ivan D. Dobrev,* Sudarsanan Varaprath,‡ Kathleen P. Plotzke,‡ and Mark J. Utell†

**Quantitative and Computational Toxicology Group, Center for Environmental Toxicology and Technology, Colorado State University, Fort Collins, Colorado 80523; †University of Rochester Medical Center, Departments of Medicine and Environmental Medicine, Pulmonary/Critical Care Division, Rochester, New York 14642; and ‡Toxicology, Health and Environmental Sciences, Dow Corning Corporation, Midland, Michigan 48686*

Received July 16, 2002; accepted November 13, 2002

In a recent pharmacokinetic study, six human volunteers were exposed by inhalation to 10 ppm ^{14}C-D_4 for 1 h during alternating periods of rest and exercise. Octamethylcyclotetrasiloxane (D_4) concentrations were determined in exhaled breath and blood. Total metabolite concentrations were estimated in blood, while the amounts of individual metabolites were measured in urine. Here, we use these data to develop a physiologically based pharmacokinetic (PBPK) model for D_4 in humans. Consistent with PBPK modeling efforts for D_4 in the rat, a conventional inhalation PBPK model assuming flow-limited tissue uptake failed to adequately describe these data. A refined model with sequestered D_4 in blood, diffusion-limited tissue uptake, and an explicit pathway for D_4 metabolism to short-chain linear siloxanes successfully described all data. Hepatic extraction in these volunteers, calculated from model parameters, was 0.65 to 0.8, i.e., hepatic clearance was nearly flow-limited. The decreased retention of inhaled D_4 seen in humans during periods of exercise was explained by altered ventilation/perfusion characteristics during exercise and a rapid approach to steady-state conditions. The urinary time course excretion of metabolites was consistent with a metabolic scheme in which sequential hydrolysis of linear siloxanes followed oxidative demethylation and ring opening. The unusual properties of D_4 (high lipophilicity coupled with high hepatic and exhalation clearance) lead to rapid decreases in free D_4 in blood. The success of D_4 PBPK models with a similar physiological structure in both humans and rats increases confidence in the utility of the model for predicting human tissue concentrations of D_4 and metabolites during inhalation exposures.

Key Words: **octamethylcylcotetrasiloxane; D_4; inhalation pharmacokinetics; PBPK modeling; vapor retention; flow-limited metabolism; lipid sequestration.**

This work was supported in part by the Silicones Environmental, Health, and Safety Council and the National Institute of Environmental Health Sciences, National Institutes of Health. The contents of this article are solely the responsibility of the authors and do not necessarily represent the official view of the NIEHS, NIH.

[1] To whom correspondence should be addressed at Center for Environmental Toxicology and Technology, Colorado State University, Fort Collins, CO 80523. Fax: (970) 491-8304. E-mail: mreddy@colostate.edu.

Octamethylcyclotetrasiloxane (D_4), a silicone fluid with a molecular weight of 296, is an additive in personal care products, an ingredient in high-performance cleaning products, and an intermediate in the production of silicone polymers. Repeated inhalation exposures of Fischer 344 (F344) rats to D_4 resulted in the induction of CYP 2B family enzymes and epoxide hydrolase in the liver, a pattern similar to the enzyme induction profile for phenobarbital. Exposure to D_4 also produced hepatomegaly, transient hepatic hyperplasia, and sustained hypertrophy in rats in a manner similar to that resulting from phenobarbital exposure (McKim *et al.,* 2001). The general population may be exposed to low levels of D_4 by the dermal and inhalation exposure routes, and workplace exposures may occur by inhalation during the production of D_4 or silicone polymers.

Plotzke *et al.* (2000) studied the disposition of D_4 in the rat following inhalation exposures. Groups of male and female F344 rats were exposed for 6 h to 7, 70, or 700 ppm ^{14}C-D_4 and tissues were collected at 10 different times during and after the exposures. In addition, other groups of rats were exposed to 7 and 700 ppm D_4 for 15 days to determine the effect of multiple exposures on D_4 pharmacokinetics. These data served as the basis for developing a physiologically based pharmacokinetic (PBPK) model for D_4 in rats. Andersen *et al.* (2001) found that a conventional PBPK model structure including flow-limited uptake in the fat, liver, and rapidly and slowly perfused tissue compartments could not adequately describe the pharmacokinetics of D_4 in rats. Specifically, this conventional model structure could not simultaneously describe the concentrations of D_4 in the blood and exhaled air in the postexposure period with a single set of physiological parameters and partition coefficients. Some D_4 appeared to be present in blood in a form that was not available for equilibration followed by exhalation in the alveolar region of the lung. A refined PBPK model was developed that included deep-tissue compartments in the liver and lung, a second fat compartment, and a storage compartment in blood from which D_4 was not available for gas or tissue exchange. This storage compartment in blood is likely

TABLE 1
Physiological Parameters and Exposure Concentrations for Subjects of Two Studies

		Utell (2000)							Utell *et al.* (1998)	
	Period	Subj. 1	Subj. 2	Subj. 3	Subj. 4	Subj. 5	Subj. 6	Average[a]	Men (average)[a,b]	Women (average)[a,b]
Age (years)		52	51	34	35	24	42	39.7 ± 10.8	32.4 ± 9.5	35.5 ± 4.0
Body weight (kg)		91	74	75	76	75	83	79.0 ± 6.7	70.9 ± 10.9	69.5 ± 9.7
Exposure conc. (ppm)		10.4	10.3	10.0	9.96	7.82	8.89	9.56 ± 1.01	10.3 ± 0.4	9.75 ± 0.51
Average tidal volume (l)	Rest 1	0.76	0.61	0.73	0.74	0.73	0.98	0.76 ± 0.12	0.71 ± 0.15	0.63 ± 0.11
Dead space (l)[c]		0.25	0.20	0.24	0.25	0.24	0.33	0.25 ± 0.04	0.24 ± 0.05	0.21 ± 0.04
Average minute volume (l/min)										
	Rest 1	11.8	9.64	12.0	11.5	10.6	12.9	11.4 ± 1.1	11.2 ± 1.3	10.4 ± 3.5
	Exer. 1	38.3	22.1	39.9	38.1	39.1	51.6	38.2 ± 9.4	34.8 ± 4.2	31.5 ± 9.5
	Rest 2	15.4	11.7	14.7	14.6	8.47	20.2	14.2 ± 3.9	13.2 ± 1.6	13.1 ± 3.9
	Exer. 2	42.6	25.2	39.4	35.0	29.3	59.1	38.4 ± 12.0	32.9 ± 3.9	33.0 ± 9.3
	Rest 3	22.1	12.4	17.1	16.0	11.3	24.6	17.3 ± 5.3	14.8 ± 1.9	14.9 ± 2.7
	Postexp.	16.1	11.1	11.6	11.5	7.72	14.9	12.2 ± 3.0	11.3 ± 1.3	11.0 ± 3.5
Average QP (l/min)[d]										
	Rest 1	7.83	6.45	8.01	7.69	7.04	8.57	7.6 ± 0.7	7.4 ± 0.9	7.0 ± 2.4
	Exer. 1	33.5	18.7	35.1	33.0	32.3	43.7	32.7 ± 8.0	29.7 ± 3.5	26.3 ± 8.5
	Rest 2	10.9	8.27	10.5	10.6	4.3	14.5	9.9 ± 3.4	9.1 ± 1.2	8.9 ± 2.7
	Exer. 2	36.8	21.7	34.2	29.6	23.0	49.7	32.5 ± 10.3	27.7 ± 3.4	27.5 ± 7.8
	Rest 3	16.6	8.97	12.5	11.7	6.33	17.9	12.3 ± 4.4	10.6 ± 1.6	10.5 ± 1.6
	Postexp.	11.3	7.56	7.55	7.58	3.73	9.08	7.8 ± 2.5	7.5 ± 1.3	7.5 ± 1.8
Resting QC (l/min)[e]		5.03	5.08	6.29	6.20	7.33	5.66	5.9 ± 0.9	6.5 ± 0.8	6.2 ± 0.4
Exercising QC (l/min) [f]		8.09	8.19	10.1	9.99	11.8	9.12	9.6 ± 1.4	10.5 ± 1.3	9.9 ± 0.6

[a]Average values are reported as mean ± one SD.
[b]Eight men and four women participated in this study.
[c]Estimated as one-third the average tidal volume during the first rest period.
[d]Calculated as the minute volume minus the dead space times the respiration rate.
[e]Calculated using the correlation (Brown *et al.,* 1997): QC, l/min = −6.846 log (age, years) + 16.775.
[f]Estimated as 160% of resting QC.

related to circulating lipids (Andersen *et al.,* 2001); however, studies have not been done to track D_4 in blood lipids over time after an inhalation exposure.

Because of the low order of D_4 toxicity, two pharmacokinetic studies of D_4 inhalation in humans have been performed in which volunteers were exposed to 10 ppm D_4 during alternating periods of rest and exercise. In the more comprehensive of the two studies, ^{14}C-D_4 was administered and the concentration of parent compound in the blood and exhaled breath and the amount of metabolite in the blood and urine were determined (Utell, 2000). In this article we describe a PBPK model developed for D_4 inhalation exposures in humans using these pharmacokinetic data. Adopting the strategy of Andersen *et al.* (2001), we first developed a simple PBPK model for human inhalation exposures to D_4 and added additional components as necessary. The resulting refined human PBPK model that successfully described the data with the radiolabeled D_4 was then validated by successfully predicting blood and exhaled breath levels for an earlier pharmacokinetic study of D_4 in human volunteers conducted with unlabelled D_4 (Utell *et al.,* 1998). Our success in developing a consistent PBPK model with common physiological structure for both rats and humans indicates that this model should be useful for assessing tissue exposures from inhaled D_4 in humans for a variety of exposure situations and supporting human risk assessments for this compound.

MATERIALS AND METHODS

Experimental data. The pharmacokinetic study on the inhalation exposure of humans to D_4 (Utell, 2000) was completed at the University of Rochester following the approval of the Human Subject Review Committee. During a 1-h exposure to 10 ppm ^{14}C-D_4 using a mouthpiece exposure system described previously (Utell *et al.,* 1998), six male volunteers rested for 10 min, exercised for 10 min, rested for 20 min, exercised for 10 min, and then rested for 10 min. For exercise, the subjects biked at a resistance that tripled their resting minute ventilation. For each subject, the respiration rate and minute volume were determined during the exposure (Table 1). The D_4 concentration in the inhaled and exhaled air was monitored regularly during the exposure, and the exhaled concentration was monitored during a 20 to 30-min postexposure period. Samples of expired breath were also obtained at 1, 3, 6, 24, 48, and 72 h after the exposure ended by the collection of end-expiratory air in a 40-l Tedlar bag. Blood samples were drawn from the forearms of each subject at 0, 30, 60, 120, 240, 420, and 1500 min after the exposure began. At the end of the 30-min postexposure period, a spot urine sample was collected and each subject emptied his bladder. For the remainder of the 24 h following the exposure, subjects collected urine in three 8-h aliquots. After the first 24 h, spot urine samples were collected once a day for up to seven days and adjusted for the total amount eliminated based on the amount of creatinine in the urine samples.

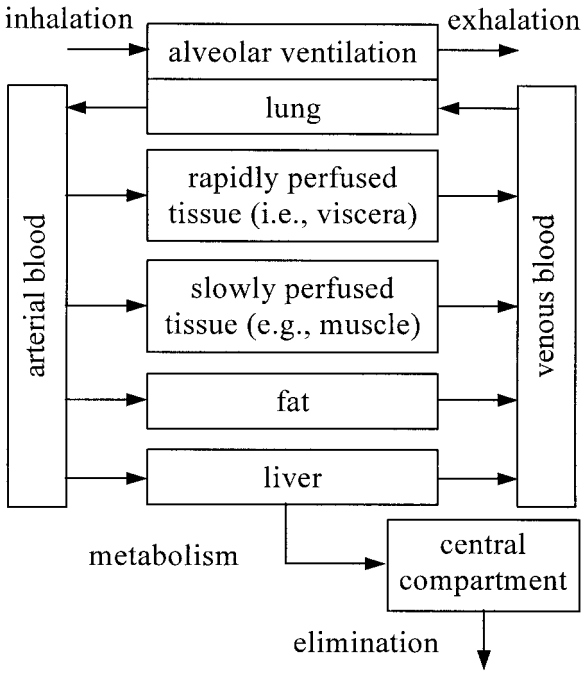

FIG. 1. Schematic diagram of the simple PBPK model for D_4 distribution in humans.

Several analytical techniques were used to measure D_4 and metabolite concentrations in various samples. During the exposure and 30-min postexposure periods, the analysis of D_4 in the exhaled breath was determined using a gas chromatograph (GC) with a flame ionization detector (FID). Samples of exhaled breath taken after the 30-min postexposure period were passed through an adsorbent for trapping volatiles and then through a CO_2 absorbent to determine the amount of ^{14}C-CO_2 separately from the radioactivity associated with volatile parent or metabolites. In rats, all radioactivity captured in the volatile trap was parent compound (Plotzke *et al.,* 2000), and the same was expected to be true for humans (i.e., chemical trapped in the volatile trap can be assumed to be parent D_4). Liquid scintillation counting (LSC) was used to determine the amount of ^{14}C-D_4 and ^{14}C-CO_2 in samples of exhaled breath collected more than 30 min after the exposure ended. Whole blood and blood plasma samples were analyzed with the LSC and gas chromatography/mass spectrometry (GC/MS, as described by Varaprath *et al.,* 2000) analytical techniques. The amount of total metabolites in the blood can be calculated by subtracting the amount of parent compound measured by GC/MS from the amount of radioactivity measured by LSC (i.e., parent compound and metabolite). Urine samples were analyzed using LSC. Additionally, individual metabolites in urine were separated using high-performance liquid chromatography (HPLC) and quantitatively analyzed using LSC.

Model structure. Initially, a fairly conventional PBPK model, as used by Ramsey and Andersen (1984) with styrene, was used to describe D_4 disposition in humans with flow-limited uptake in the fat, liver, and rapidly and slowly perfused tissues, along with separate compartments for the venous and arterial blood (Fig. 1). In the simple model, all the D_4 in the blood was available for equilibration with tissues and lung air. In the rat the rate of metabolism had been modeled by a Michaelis-Menten term in the liver and included provision for induction of metabolism at 700 ppm D_4. Because the human subjects were exposed to only 10 ppm D_4, metabolism was described with dose-independent liver clearance without provision for induction. The conventional model structure also included a one-compartment pharmacokinetic model for a combined metabolite pool in blood.

In the rat, PBPK modeling results indicated that some D_4 in the blood was unavailable for exchange with exhaled air and the amount of D_4 in this pool varied with time (Andersen *et al.,* 2001). The successful model in the rat had deep tissue compartments and a pool of D_4 in blood that was unavailable for exhalation or tissue uptake. A second refined PBPK model was developed with the human data to determine if such an elaboration on the conventional model structure was also necessary to account for human kinetics. The refined model (Fig. 2) included a blood pool of unavailable D_4. As with the rat model, this unavailable pool of D_4 was assumed to be produced in the liver, transported in the blood, and cleared by the fat tissue. This behavior is representative of lipoprotein transport. A mass transfer resistance was required to describe the uptake of D_4 by fat tissue in rats. In the human model we included a mass transfer resistance to uptake in the slowly perfused compartment and a deep storage compartment in fat. The role of these compartments in describing the experimental data is noted in the Results. Model equations are provided in Appendix 1 and the code is available by e-mail from the corresponding author.

Metabolism. Time course data for the amount of individual metabolites in the urine were available for the development of a more detailed model of D_4 biotransformation pathways in humans. After determining the kinetic parameters for net metabolic clearance of parent D_4, the data for the amount of individual metabolites in the urine were used to create a more complete description of the formation and clearance of individual metabolites. The proposed metabolic scheme and model structure (Figs. 3 and 4) show the expected interrelationships of the individual metabolites that were included in the model for D_4 metabolism.

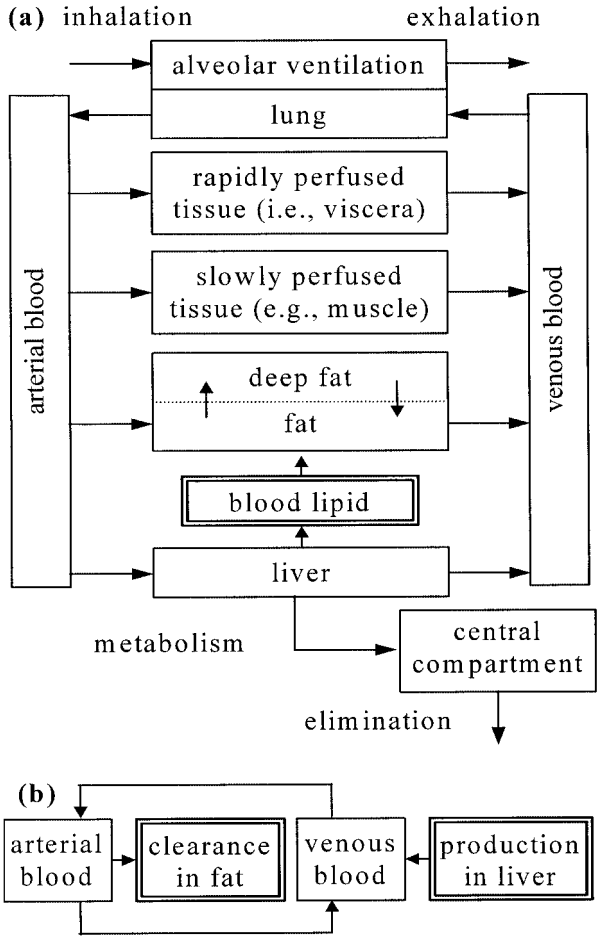

FIG. 2. Schematic diagram of (a) the refined PBPK model for D_4 distribution in humans and (b) the submodel for the transport of unavailable D_4 in blood lipids. The double line designates a variable from a component in another section of the model.

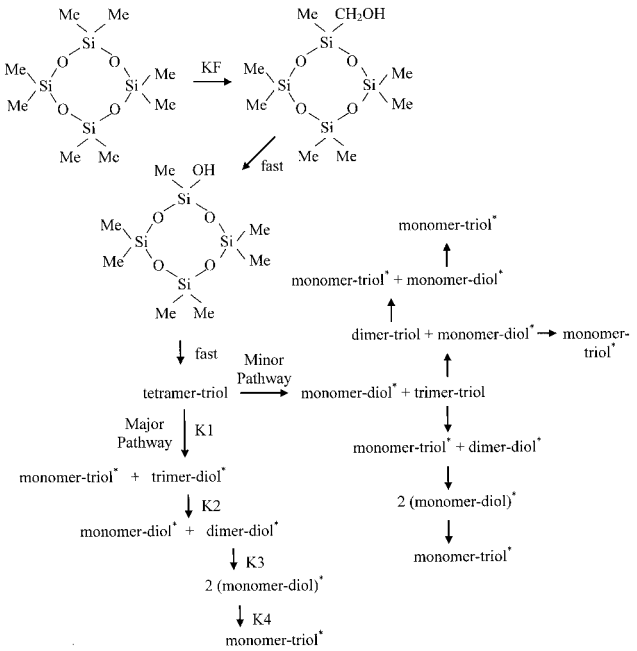

FIG. 3. Proposed reaction mechanism for D_4 metabolism in humans. *Designates compounds that were detected in urine samples.

Parameterization. A variety of physiological parameters were experimentally measured or calculated for the individual subjects of the study (Table 1). Effects of exercise were incorporated in the model by adjusting the alveolar ventilation rate, QP, the cardiac output, QC, and the blood flow rates to two tissue compartments (Table 2; see Appendix 2 for a listing of the abbreviations used in the models). During exercise, the blood flow rate to the fat compartment increased in a manner consistent with the study of Bulow and Madsen (1978), and the blood flow rate to the slowly perfused tissue compartment, which includes muscle tissue, increased during exercise. The blood flow rates to the liver and rapidly perfused tissue were the same during both the rest and exercise periods.

To minimize the number of parameters to be estimated, values of the liver:blood, fat:blood, and rapidly perfused tissue:blood partition coefficients were calculated by dividing the experimental, *in vitro*, rat-tissue values for the liver:air, fat:air, and kidney:air partition coefficients, respectively, by the blood:air partition coefficients (Andersen *et al.,* 2001). Tissue partition coefficients of rats and humans are expected to be similar because tissue compositions are similar. Because *in vitro* partitioning data were not available for the slowly perfused tissue compartment, the partition coefficient for D_4 between the slowly perfused compartment and blood, PS, was set to 3. The value of PS cannot be calculated from the *in vivo* data because fits of the model to these data (e.g., time course concentrations of D_4 in blood plasma) were not sensitive to the value of PS. This parameter did affect the estimates of the amount of chemical retained during inhalation exposure. Although no experimental data were available for the estimation of PS, the potential effect of error in this parameter is small. The slowly perfused compartment is large, but PS is small compared to the partition coefficients of other compartments, and so it stores a relatively small amount of chemical.

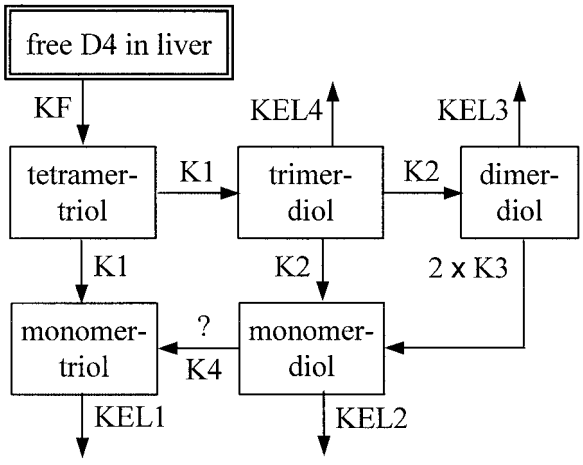

FIG. 4. Schematic diagram of the D_4 metabolism submodel.

TABLE 2
Additional Parameters Used in the PBPK Models

Parameter	Value
Fraction of blood flow to tissues	
Liver	0.227 (0.142)[a]
Fat	0.052 (0.098)[a]
Rapidly perfused tissue	0.472 (0.295)[a]
Slowly perfused tissue	0.249 (0.465)[a]
Fraction of body weight in tissues	
Liver	0.0314[b]
Fat	0.23[b]
Rapidly perfused tissue	0.05[b]
Slowly perfused tissue	0.5396[b]
Blood	0.059[b,c]
Partition coefficients	
Liver:blood	8.9[d]
Fat:blood	490[d]
Slowly perfused tissue:blood	3[e]
Rapidly perfused tissue:blood	8.4[d]

[a]The numbers in parentheses are the values during exercise periods. During exercise, blood flow rates to the rapidly perfused tissue and liver remained the same, while blood flow rates to the fat and slowly perfused compartments increased, with 21 and 79% of the increase in blood flow going to the fat and slowly perfused tissues, respectively. The increase in blood flow rate to fat was based on Bulow and Madsen (1978).

[b]From Brown *et al.* (1997). The sum of the fraction of body weight in each compartment is 0.91 because 9% of the body was assumed to receive minimal blood flow. The specific gravity of all tissues was estimated to be 1.

[c]The arterial and venous blood compartments were estimated to contain 35 and 65% of the blood volume, respectively.

[d]Calculated using blood:air and tissue:air partition coefficients measured *in vitro* in the rat from Andersen *et al.* (2001).

[e]This parameter was set to 3 for reasons discussed in Materials and Methods.

For the simple model, four parameters were estimated from the experimental data: (1) the blood:air partition coefficient (Pb), (2) the allometric scaling constant for metabolic clearance in the liver (KFC), (3) the renal clearance of metabolite into the urine (KEL), and (4) a scaling constant for the volume of distribution of the metabolite pool (VDISC). For the refined model, five additional parameters were estimated: (5) the first-order rate constant for the production of the mobile lipid pool in the liver (Kmlp), (6) the clearance of unavailable D_4 in the mobile lipid pool to the fat (CLmlp), (7) a mass transfer coefficient for the slowly perfused compartment (PAS), (8) a first-order mass transfer coefficient for the movement of D_4 from the fat compartment into a deep compartment (KFD), and (9) a first-order mass transfer coefficient for the movement of D_4 from the deep compartment to the fat compartment (KDF).

These parameters were estimated by comparing model output to the cumulative amount of chemical absorbed during the exposure, the concentration of D_4 in the exhaled breath after the exposure, the concentration of D_4 in the plasma, and the concentrations of total metabolites in the plasma and urine. Although the concentrations of D_4 and metabolites were determined in both the whole blood and the blood plasma, parameter estimation was done using blood plasma concentrations. The concentrations of individual metabolites in the urine were also used to estimate parameters for the metabolism model.

Model equations were solved using two different software packages: Berkeley Madonna™ and ACSL™ (Aegis Technologies). Optimum parameters were found using the multiple curve-fitting routine in Berkeley Madonna, which minimizes the root mean square deviation between the data points and the model output. When multiple data sets were used for parameter estimation (e.g., time course data for the amount of several different metabolites in urine), the residuals from each dataset were weighted by the inverse of the SD of the dataset since the datasets were assumed to have a constant coefficient of variance. For the refined model, after completing a global estimation of the best-fit parameters, we independently adjusted Kmlp and CLmlp to improve the fit for blood plasma concentrations taken at 1500 h and adjusted KDF to provide a better fit for exhaled breath concentrations for times longer than 1500 h. Because the concentrations in blood and exhaled breath at the longest time were more than four orders of magnitude smaller than those during exposure, the curve-fitting algorithm was relatively insensitive to these latter data points. When estimating multiple parameters by curve fitting, increasing the number of parameters to be fit increases the risk that the program will find a local minimum of residuals instead of the global minimum. To prevent identifying a combination of parameters resulting in a local optimum instead of a global optimum, the optimizer was run using several different starting values (i.e., initial guesses of parameter values). Additionally, by limiting the values of parameters to physically plausible values, unrealistic solutions were prevented and computational time was minimized (MGA Software, 1997).

Sensitivity analysis. Identification of the key parameters affecting a pharmacokinetic measurement is important for calculating multiple parameters by curve-fitting with multiple datasets (Andersen *et al.,* 2001). For example, a key parameter for determining the D_4 concentration in exhaled air and blood plasma during the exposure and washout period is Pb. By fitting this parameter independently to data that are sensitive to the parameter (i.e., holding other parameters constant), its value can be constrained for the multiple curve-fitting algorithm, reducing the computational time required by the computer and the risk of calculating an unrealistic value of the parameter based on datasets lacking sensitivity to the parameter.

To determine sensitivity of the model output to the parameters estimated using the experimental data, log-normalized sensitivity parameters (LSPs), defined in Clewell *et al.* (1994) as

$$\mathrm{LSP} = \frac{\partial \ln R}{\partial \ln x} \quad (1)$$

were calculated. In Equation 1, R is the model output (i.e., for the calculations performed here, the concentrations of D_4 in the venous blood plasma and exhaled breath) and x is the parameter for which sensitivity is being determined. By this definition, the percentage change in model output due to a percentage change in a parameter is quantified, and thus the LSP value represents the relative importance of a parameter to model output. Values of LSP were calculated using the central difference method. Because model output may be sensitive to model parameters at different times, values of LSP were calculated at four times: 30 min, 2 h, 12 h, and 48 h. Values of LSP greater than one could result in error in the input causing amplified error in the output, while very low values of LSP indicate that model output are insensitive to a parameter (Clewell *et al.,* 1994).

Model validation. A separate study in which 12 humans were exposed to 10 ppm D_4 by inhalation during periods of rest and exercise (Utell *et al.,* 1998) was used as a test set for limited model validation. In this study, the inspired D_4 vapor concentration was determined using infrared spectrophotometry. Concentrations of D_4 in the exhaled breath during the exposure and washout period were determined every 2 min by GC methods. Blood plasma D_4 concentrations during, immediately after, and 1, 6, and 24 h after the exposure ended were determined using GC/MS analysis. Plasma sample concentrations 24 h after the exposure ended were below the limit of quantitation for this analytical method.

RESULTS

General Trends

Unlike many lipophilic chemicals with long half-lives for elimination from the body, elimination of D_4 ($\log K_{o/w} = 5.1$) from blood was rapid. After humans were exposed to 10 ppm ^{14}C-D_4 by inhalation, D_4 blood concentrations decreased rapidly due to exhalation and metabolism (Table 3). In the 30-min period following the exposure, about 13% of the absorbed dose of D_4 was eliminated by exhalation. Metabolites were detected in the blood at the earliest sampling time (30 min after the exposure began), and the first urine sample taken 30 min after the exposure had ended also had detectable levels of metabolites.

Model Structure

Consistent with the pharmacokinetics of D_4 in the rat, the refined model more accurately described the disposition of D_4 in the plasma and exhaled air (Fig. 5). For example, both the simple and refined model could match the concentration of D_4 in exhaled air, but only the refined model could simultaneously match the concentration of D_4 in blood plasma and exhaled air. Simulated D_4 exhaled breath concentrations increased between 10 to 20 min and 40 to 50 min (i.e., during the exercise periods) due to the physiological changes from exercise that were incorporated in the model. This increase in exhaled D_4 concentrations is consistent with the pharmacokinetic study results of Utell *et al.* (1998), who noted decreased retention efficiency of D_4 during the exercise periods.

Average values of D_4 concentrations in exhaled breath and plasma, total metabolite concentration in the plasma, and cumulative amount of metabolite in the urine for the six subjects exposed to ^{14}C-D_4 are shown in Figure 6. The simulated curves were calculated using the average values of the inhaled D_4 concentration and physiological properties (Table 1) and the average values of calculated model parameters (Table 4). Although model calculations are presented for average parameter values, parameter values for each individual subject are reported to illustrate the interindividual variability in parameter values. As expected, the refined model more accurately described the pharmacokinetic profiles. Although the model prediction of the D_4 concentration in exhaled breath is high during the first 500 min postexposure, in general the refined model describes the concentration of D_4 in exhaled breath and blood plasma, the concentration of total metabolite in blood plasma, and the cumulative amount of metabolite in the urine.

After the exposure ended, the D_4 concentration in exhaled breath, Cex, decreased by more than four orders of magnitude.

TABLE 3
Summary of D_4 Absorption, Metabolism, and Excretion

Measured quantity	Time of estimation	Data[a]	Simple model	Refined model
Amount that entered the lungs (mg)	End of exposure (60 min)	154 ± 39	158 ± 38	158 ± 38
Amount retained (mg)	End of exposure (60 min)	19 ± 6	17 ± 3	14 ± 2
Concentration of D_4 in plasma (μg/l)				
	End of exposure (60 min)	115 ± 50	60 ± 14	121 ± 39
	1 day postexposure	3.1 ± 2.9	0.028 ± 0.014	1.8 ± 1.3
Concentration of metabolites in plasma (μg D_4 eq./l)				
	End of exposure (60 min)	56 ± 18	38 ± 13	41 ± 15
	1 day postexposure	29 ± 9	30 ± 14	27 ± 8
Cumulative amount of D_4 exhaled after exposure ended (mg)				
	30-min period following the exposure	2.5 ± 0.6	3.1 ± 1.2	2.7 ± 1.1
	8 days following the exposure	ND[b]	9.9 ± 2.1	5.7 ± 1.7
Cumulative amount of D_4 metabolites excreted in urine (mg D_4 eq.)				
	1 day postexposure	2.2 ± 0.3	2.0 ± 0.4	2.1 ± 0.5
	8 days postexposure	5.0 ± 0.9[c]	5.3 ± 1.7[c]	4.6 ± 0.9[c]

[a]Average values ± one SD for $n = 6$.
[b]ND, not determined.
[c]Data were only available for Subjects 4 through 6, and so the average simulated value only included Subjects 4 through 6 for a fair comparison.

During the exposure, the prime determinant of plasma concentration was Pb (Table 5). At the later times, the return of D_4 to plasma from the lipophilic storage tissues in the body was also a prime determinant of the concentration of D_4 in exhaled air. While the overall time course for Cex, with the precipitous decline over time, was accounted for by the simple model (Fig. 6), the curve decreased too rapidly and leveled off at a concentration higher than the data. With this simple model, the characteristics of the slowly perfused compartment, representing muscle and skin, determined the curvature between 100 and 1500 min.

Describing the exhalation time course data more accurately

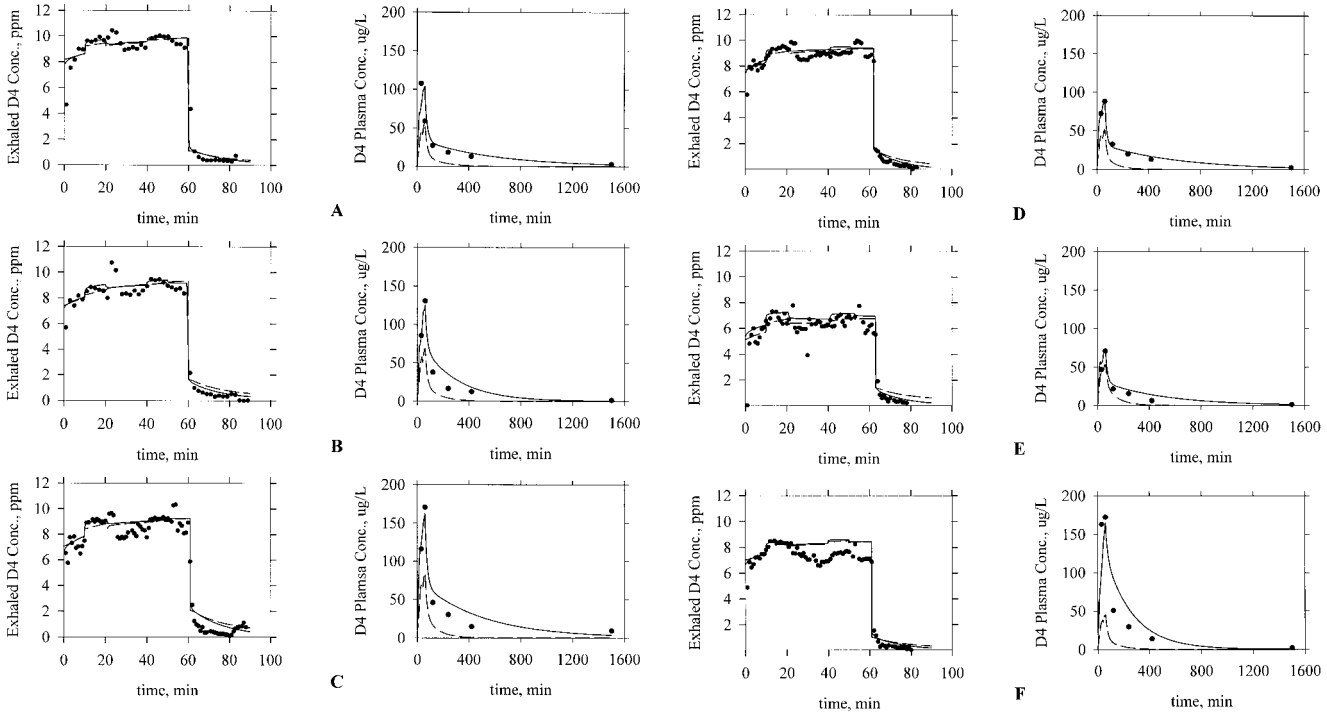

FIG. 5. Measured and calculated D_4 concentrations in exhaled breath and blood plasma as a function of time for subjects (A) 1, (B) 2, (C) 3, (D) 4, (E) 5, and (F) 6 of the primary study. Theoretical curves were calculated with the simple (dashed curve) and refined (solid curve) models.

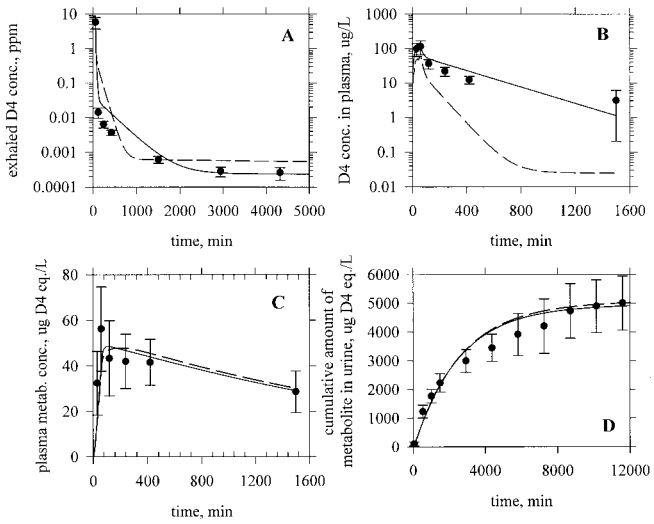

FIG. 6. Semilog plots of the average concentration of D_4 in (A) exhaled breath and (B) blood plasma and plots of (C) the concentration of total metabolite in blood plasma and (D) the average cumulative amount of total metabolite in urine as a function of time. The error bars represent one SD for $n = 5$ or 6. The simulated curves were calculated using the refined model (solid curves) and simple model (dashed curves) with average best-fit parameters, physiological properties, and exposure conditions.

required the addition of diffusion limitations in storage for both the slowly perfused and the fat compartments of the refined model. Several characteristics of the refined model dominated the behavior in different time periods. The characteristics of the slowly perfused compartment were critical in fitting the transitional period until about 1000 min and required incorporation of a mass-transfer limitation on uptake and release of chemical from this compartment. After about 2000 min, the more stable blood level of D_4 was determined by return from the fat compartment. If a flow-limited fat compartment without a deep compartment were included, the model overestimated the exhaled concentrations at longer times as shown by the dotted line. The presence of a diffusion-limited fat compartment allowed adjustment of the model fit for the final period of exhalation after 3000 min. The exhalation behavior of D_4 is a sensitive monitor of the characteristics of lipid storage compartments because of the rapid clearance of D_4 by exhalation and metabolism after its release from storage sites. Further refinements in the fit to the exhaled breath curve were possible by subdividing the slowly perfused compartment (e.g., as in Jonsson *et al.,* 2001). We did not believe that an increase in model complexity was warranted by the limited data available from the single exhaled breath data set.

Model Validation

The refined model was then applied to a second data set (Utell *et al.,* 1998). Using average characteristics and exposure conditions of the eight male and four female subjects as input for the model (Table 1), concentrations of D_4 in exhaled breath and blood plasma were simulated for male and female subjects

TABLE 4
Parameters Calculated by Fitting the Model to the Data Obtained following Inhalation Exposures of Six Male Subjects to ^{14}C-D_4

	Subject						
Parameters	1	2	3	4	5	6	Average[a]
Simple model							
Pb	0.72	0.89	1.0	0.63	1.02	0.69	0.83 ± 0.17
KFC(l/min/kg$^{0.7}$)[b]	0.071	0.065	0.047	0.090	0.2[d]	0.2[d]	0.11 ± 0.12
KEL (l/min)	0.055	0.038	0.045	0.039	0.020	0.026	0.037 ± 0.013
VDISC (l/kg)[c]	0.87	1.82	1.2	0.98	1.6	0.82	1.2 ± 0.4
Refined model							
Pb	0.92	1.0	1.3	0.75	0.86	0.90	0.96 ± 0.19
KFC (l/min/kg$^{0.7}$)[b]	0.052	0.11	0.036	0.065	0.2[d]	0.12	0.097 ± 0.060
KEL (l/min)	0.057	0.033	0.041	0.036	0.033	0.029	0.038 ± 0.010
VDISC (l/kg)[c]	1.0	2.5	1.1	0.88	1.1	0.70	1.2 ± 0.6
Kmlp (1/min)	0.020	0.060	0.022	0.022	0.044	0.15	0.053 ± 0.050
CLmlp (l/min)	0.010	0.018	0.010	0.0080	0.010	0.025	0.014 ± 0.007
KFD (1/min)	0.0043	0.0028	0.0019	0.0019	0.0078	0.0043	0.0038 ± 0.0022
KDF (1/min)	0.0015	0.002	0.001	0.0012	0.0019	0.0050	0.0021 ± 0.0015
PAS (l/min)	0.30	0.61	0.30	0.33	0.43	0.21	0.36 ± 0.14

[a]Average for six subjects ± one SD.
[b]Metabolic clearance in the liver, KF, is calculated as KFC × BW$^{0.7}$.
[c]The volume of distribution for the combined metabolite pool, VDIS, is calculated as VDISC × BW.
[d]KFC was high enough that the rate of metabolism was controlled by blood flow to the liver and KFC could not be calculated from the data for this subject. The value of KFC was set so that the average value of KFC resulted in the model matching the average cumulative amount of metabolite in the urine eight days after the exposure had ended.

TABLE 5
Summary of the Log-Normalized Sensitivity Parameter Values for D_4 Concentrations

	In blood plasma				In exhaled air			
	30 min	2 h	12 h	48 h	30 min	2 h	12 h	48 h
PB	0.84	0.95	0.99	1.3	–0.097	1.1	0.83	0.69
KFC (l/min/kg$^{0.7}$)	–0.17	–0.59	–0.61	–0.54	–0.014	–0.13	–0.060	–0.11
Kmlp (1/min)	0.23	0.91	0.94	0.79	~ 0	~ 0	0.097	0.072
CLmlp (l/min)	~ 0	–0.20	–1.7	–3.4	~ 0	~ 0	~ 0	~ 0
KFD (1/min)	~ 0	~ 0	~ 0	–0.33	~ 0	~ 0	–0.032	–0.59
KDF (1/min)	~ 0	~ 0	~ 0	0.33	~ 0	~ 0	0.026	0.59
PAS (l/min)	–0.075	0.026	0.052	–0.34	–0.016	0.75	0.16	–0.32

Note. The sensitivity analysis was not performed for parameters KEL and VDISC because the calculated values of concentrations of D_4 in the blood plasma and exhaled breath are not affected by these parameters. Values of LSP between –0.01 and 0.01 were reported as ~ 0.

using the average parameter values of the refined PBPK model (Table 4). The prediction (Fig. 7) agrees very well with these earlier results. However, since this dataset is similar to the data used for model construction, it might be better to regard this as test of reproducibility rather than a strict validation of the model. Although the model parameters were estimated using data from a study of six male subjects, the model was able to predict exposure outcomes for female subjects of the previous study.

Metabolism Model

Consistent with metabolism studies performed in the rat (Varaprath *et al.,* 1999), methylsilanetriol (monomer-triol) and dimethylsilanediol (monomer-diol) were the major metabolites in humans (Fig. 8). Other metabolites in urine common to both rat and human metabolism of D_4 were tetramethyldisiloxane-1,3-diol (dimer-diol), dimethyldisiloxane-1,3,3,3-tetrol (dimer-tetrol), and hexamethyltrisiloxane-1,5-diol (trimer-diol; Table 6). Additionally, trimethyldisiloxane-1,3,3-triol (dimer-triol) was a very minor metabolite in human urine. Although the exact mechanism of D_4 metabolism is unknown, these metabolites can be incorporated into a proposed scheme for metabolism (Fig. 3) and assigned compartments in a metabolism model (Fig. 4). In all the proposed pathways, complete hydrolysis leads to 1 mol of monomer-triol and 3 mol of monomer-diol. However, intermediates may also be filtered into urine. Large quantities of monomer-triol were detected in the urine soon after the exposure ended, indicating that the reaction of tetramer-triol to form monomer-triol and trimer-diol is likely to be the major pathway for metabolism.

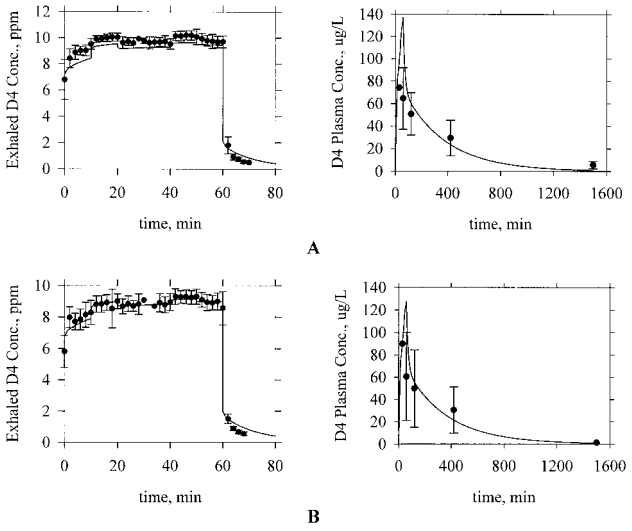

FIG. 7. Average measured and calculated D_4 concentrations in exhaled breath and blood plasma as a function of time for (A) the men (n = 8) and (B) women (n = 4) from Utell *et al.* (1998). Simulated curves were calculated with the refined model. The error bars represent one SD.

One potential problem with the mechanism shown in Figure 3 is that dimer-tetrol does not appear in the mechanism. The formation of dimer-tetrol could be explained by another minor pathway. During the initial step of the oxidation of D_4, if both methyl groups on an Si were oxidized, silicic acid, i.e., $Si(OH)_4$, could be formed. In the urine, which has a higher concentration of metabolites than the blood, a condensation reaction between silicic acid and monomer-diol could produce dimer-tetrol.

During the primary study, $^{14}C\text{-}CO_2$ was detected in exhaled breath in concentrations that decreased exponentially and reached very low levels by 24 h after the exposure ended. It is likely that $^{14}C\text{-}CO_2$ was produced from the oxidation of the methyl group from the intact D_4 molecule (i.e., the first step in the metabolic pathway). Eight days after the exposure ended, about 26% of the D_4 had been eliminated by metabolism. Because only one of the methyl groups on the D_4 molecule is radiolabeled, about 3.25% (= 26%/8) of the radioactivity should be eliminated in the form of $^{14}C\text{-}CO_2$, but only about 1.5% of the uptake of radioactivity was recovered as $^{14}C\text{-}CO_2$. The exhaled breath was not analyzed for $^{14}C\text{-}CO_2$ during the exposure and the 30-min postexposure period. Thus, more than half of the $^{14}C\text{-}CO_2$ from the initial oxidation of D_4 could have

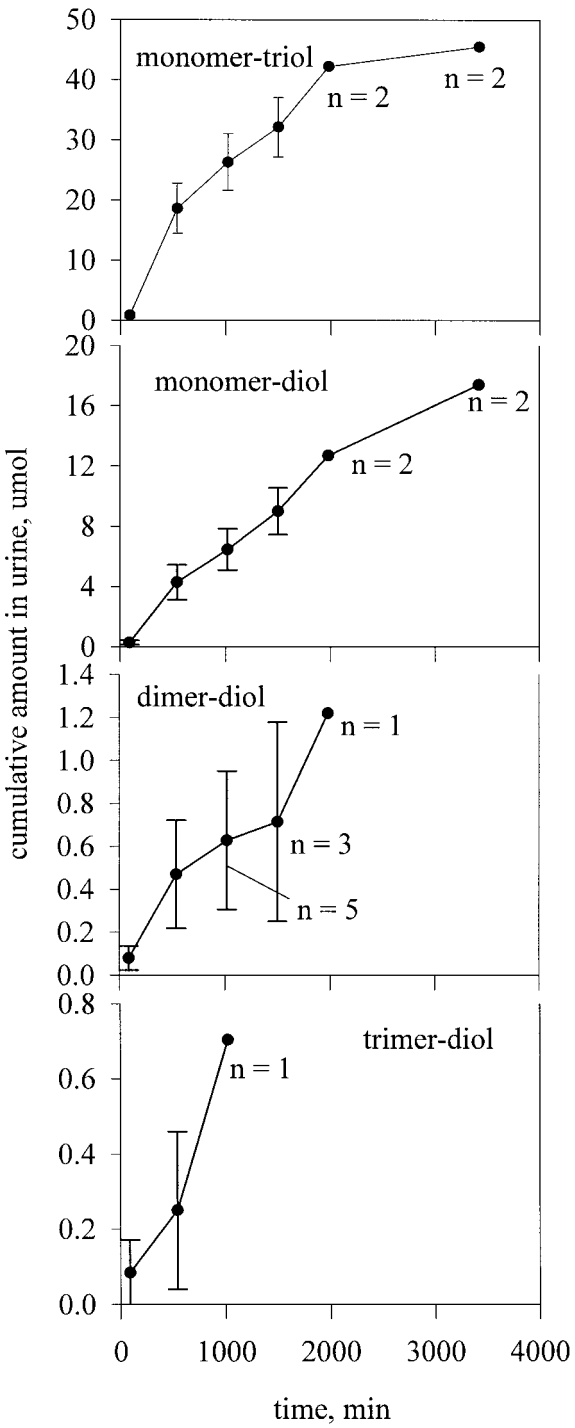

FIG. 8. Average cumulative amounts in μmol of five metabolites in urine as a function of time. The error bars represent one SD. Unless otherwise indicated, $n = 6$. Points are connected; the line does not represent model simulation.

been eliminated without detection. Because less than 5% of the total radioactivity will be metabolized to ^{14}C-CO_2, this loss was not expected to significantly affect modeling results, and was not included in the model development.

The submodel for metabolism of D_4 in humans (Fig. 4), developed to be consistent with the major pathway of the proposed reaction mechanism (Fig. 3), was then combined with the refined PBPK model. The equations are provided in Appendix 1. The metabolism submodel required values for seven additional parameters: the allometric scaling constants for the first-order metabolism rate constants of tetramer-triol, trimer-diol, and dimer-diol (i.e., K1C, K2C, and K3C, respectively) and the first-order rate constants for the elimination of monomer-triol, monomer-diol, dimer-diol, and trimer-diol into urine (i.e., KEL1, KEL2, KEL3, and KEL4, respectively). These seven parameters were determined by minimizing the difference between model output and six datasets (i.e., the cumulative amount of monomer-triol, monomer-diol, dimer-diol, and trimer-diol in urine, the cumulative amount of total metabolite in urine, and the concentration of total metabolites in plasma). Parameter estimation results are listed in Table 7.

This metabolism submodel adequately described time course concentrations of three of the four individual metabolites in urine (i.e., monomer-diol, dimer-diol, and trimer-diol; Fig. 9). However, the model underpredicted the cumulative amount of monomer-triol in the urine at later times by up to 56%. It appears that further oxidative demethylation must occur after formation of the linear siloxanes to account for the net amounts of monomer-triol found in urine. The model structure was enlarged to include conversion of monomer-diol to monomer-triol (i.e., the model shown in Figure 4 was modified to include an additional reaction with rate constant K4). The expanded model was able to describe all the metabolite data (Fig. 9).

DISCUSSION

Discovering the Requirement for the Refined Model

For volatile organic compounds, the ratio of the chemical concentration in arterial blood, Ca, to the concentration in end-alveolar air, Calv, is expected to remain constant (i.e., Ca/Calv = Pb). In the D_4 study, blood samples were obtained from the venous blood, and a similar time-independent relationship is expected after the exposure ends. The equation often used to calculate Ca in PBPK models (e.g., the approach of Ramsey and Andersen, 1984, for inhalation exposures to styrene) is

$$Ca = \frac{QP \times Cin + QC \times Cv}{QC + QP/Pb} \quad (2)$$

where Cin is the concentration of chemical in the air entering the lungs and Cv is the concentration of chemical in the venous return. Equation 2 was developed by assuming that the absorbed chemical rapidly equilibrates between lung blood and lung air. Because Pb = Ca/Calv and after an exposure ends, Cin = 0, the following relationship can be derived:

TABLE 6
D_4 Metabolites Identified in Human Urine

Label	Chemical name	Chemical formula
Trimer-diol	Hexamethyltrisiloxane-1,5-diol	$Me_2Si(OH)$-O-$SiMe_2$-O-$Si(OH)Me_2$
Dimer-diol	Tetramethyldisiloxane-1,3-diol	$Me_2Si(OH)$-O-$Si(OH)Me_2$
Dimer-triol	Trimethyldisiloxane-1,3,3-triol	$Me_2Si(OH)$-O-$Si(OH)_2Me$
Dimer-tetrol	Dimethyldisiloxane-1,3,3,3-tetrol	$Me_2Si(OH)$-O-$Si(OH)_3$
Monomer-diol	Dimethylsilanediol	$Me_2Si(OH)_2$
Monomer-triol	Methylsilanetriol	$MeSi(OH)_3$

$$\frac{Cv}{Calv} = Pb + \frac{QP}{QC}. \quad (3)$$

After the exposure, the ratios Cv/Calv and also Cv/Cex should have remained constant, but did not (Fig. 10). The ratio Cv/Cex increased substantially with time from about 5 soon after the exposure ended to over 400 one day after the exposure ended. This increase in Cv/Cex occurred over a time period where the blood concentrations decreased by two orders of magnitude while the exhaled air concentrations decreased by more than four orders of magnitude.

The reason that blood concentrations did not fall as rapidly as the exhaled air concentrations was the presence of a pool of D_4 in blood that did not equilibrate with exhaled air, i.e., a pool of bound or sequestered D_4 that was unavailable for alveolar equilibration. Free D_4 was rapidly exhaled or metabolized; the bound D_4 was persistent in blood. The time evolution of the amount in this nonexchangeable blood compartment determined the values of Kmlp and CLmlp. According to model calculations, when the exposure ended the fraction of D_4 in the blood that was unavailable was 0.24, but by 1 h following the exposure the fraction of unavailable D_4 had increased to 0.95.

TABLE 7
Metabolism Model Parameter Estimation Results

	Parameters	
	When K4 = 0	When K4 ≠ 0
K1C (l/min/kg$^{0.7}$)	0.14	> 0.3
K2C (l/min/kg$^{0.7}$)	0.063	0.035
K3C (l/min/kg$^{0.7}$)	0.011	0.017
K4C (l/min/kg$^{0.7}$)	—	0.0045
KEL1 (l/min)	> 0.3[a]	> 0.3[a]
KEL2 (l/min)	0.022	0.040
KEL3 (l/min)	0.027	0.040
KEL4 (l/min)	0.083	0.046

Note. Parameters were calculated both with and without an extra demethylation step (see Fig. 4).

[a]This parameter could not be calculated because the rate of mass transfer of monomer-triol into the urine was controlled by the rate of production of monomer-triol.

Consistent with the results of Utell *et al.* (1998), calculations with the refined model show that the half-life for D_4 clearance from the blood was shorter at early times than late times because the fraction of available D_4 in the blood decreased with time. When the exposure ended and the majority of D_4 in the blood was free D_4, the half-life for clearance of D_4 from the blood was about 1.4 h. However, later in the exposure when the majority of the D_4 in the blood was unavailable, the half-life for clearance was about 4.2 h. Due to the high sensitivity of blood concentrations at long times to CLmlp (Table 5), additional studies characterizing the nature of the pools of unavailable D_4 in blood are important.

The model structure for D_4 inhalation exposures in humans is perhaps more complex than warranted by the data because no tissue time-course concentration data were available. However, the model structure is also based on our experience in modeling D_4 pharmacokinetics in the rat. The premise in developing the PBPK model with D_4 in the rat was the assumption that the exhaled air D_4 was in equilibrium with a pool of free D_4 in blood. With this human model we retained the model structure required in the rat (i.e., the mobile-lipid pool

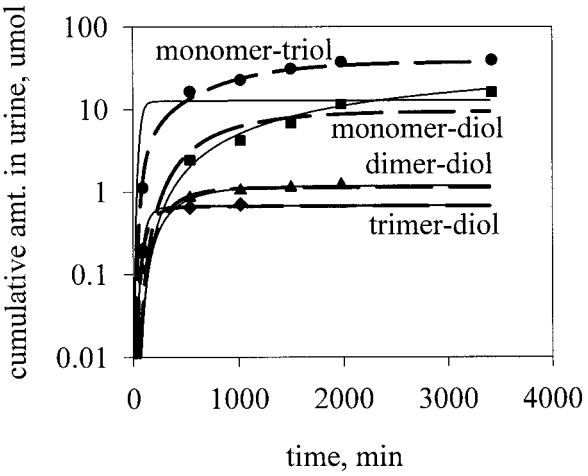

FIG. 9. Measured and calculated cumulative amount in μmol of four individual metabolites in urine as a function of time for Subject 1. The simulated curves were calculated using the refined model modified to include metabolism. For the solid curves, K4 = 0, but the dashed curves were calculated including an additional demethylation step.

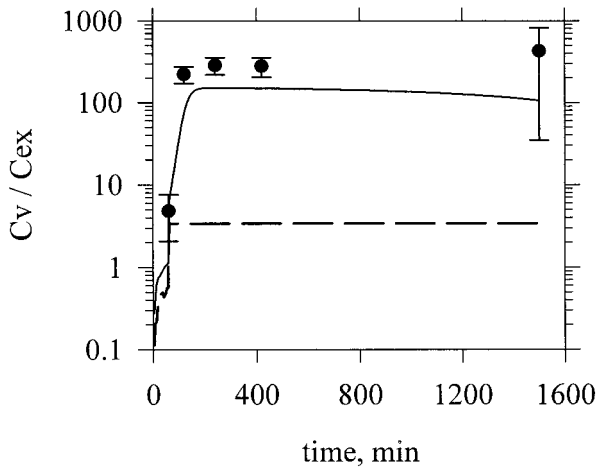

FIG. 10. Average values of Cv/Cex as a function of time. The error bars represent one SD for $n = 6$. The simulated curves were calculated using the refined model (solid curve) and simple model (dashed curve) with average best-fit parameters, physiological properties, and exposure conditions.

concept with production from the liver, movement through the plasma, and clearance to the fat). Further research will be necessary to identify the plasma lipids that sequester D_4.

Clearance of Circulating D_4

Although D_4 has a large fat:blood partition coefficient, it is not expected to undergo extensive bioaccumulation due to rapid clearance from the body by exhalation and metabolism. With xenobiotic compounds, elimination processes are frequently described by clearances (i.e., the volume of blood from which chemical is lost per time, with units of flow). With D_4, we can calculate clearances by the two major pathways of elimination, exhalation and hepatic clearance. Based on the average values of KFC (Table 4) and liver blood flow (Table 2), the average liver clearance was 0.85 l/min compared to a liver blood flow of 1.29 l/min. At the extreme, with KFC = 0.2 l/min/kg$^{0.7}$, hepatic clearance was 1.01 l/min (i.e., nearly 80% of hepatic blood flow). Under these conditions, hepatic clearance is essentially limited by blood flow to the liver.

Clearance by exhalation, CLex, can also be calculated from model parameters. In the postexposure period, CLex is calculated as

$$\mathrm{CLex} = \mathrm{QC} \times \left(\frac{\mathrm{Cv} - \mathrm{Ca}}{\mathrm{Cv}}\right). \quad (4)$$

Combining this relationship with Equation 2 for Cin = 0 gives

$$\mathrm{CLex} = \frac{\mathrm{QP}}{\mathrm{Pb} + \mathrm{QP/QC}}. \quad (5)$$

For compounds like D_4 with small values of Pb, CLex is high. For a Pb of 1.0 and resting QC and QP values of 5.03 and 7.83 l/min, CLex was 3.06 l/min. Total clearance from hepatic metabolism and exhalation was 3.91 (0.85 + 3.06) l/min (i.e., about 60% of QC).

Metabolic clearance of D_4 simply accounts for those reactions that metabolize D_4 to downstream products. Because of the ability to speciate metabolites in urine over time, it was also possible to infer the metabolic pathway for the group of linear siloxanes produced from oxidation and ring cleavage. The sequential model with rapid production of the trimer-diol after oxidation followed by hydrolysis is sufficient to describe the results as long as a second oxidative pathway is provided for conversion of monomer-diol to monomer-triol. This latter step may be more favored than oxidation of other intermediates due to longer persistence of the monomer-diol than any of the other longer chain metabolites that serve as relatively shorter-lived intermediates. This model infers time course concentrations in the blood from the appearance of metabolites in urine. The relationships of blood and urinary concentrations depend on biotransformation and elimination rates.

In rodents, inhalation of D_4 produces a dose-related hepatomegaly, transient hepatic hyperplasia, hypertrophy, and induction of cytochrome P450 enzymes in a manner similar to phenobarbital (McKim *et al.,* 1998, 2001). This pattern of induction was also observed following oral exposure to D_4 (Zhang *et al.,* 2000). Although several hepatic enzymes are affected by D_4 exposure, CYP2B1/2 enzymes are induced to the greatest extent. In addition, it appears that these enzymes are also capable of recognizing D_4 as a substrate and therefore may play an important role in its elimination (Salyers *et al.,* 1996). While there may eventually be value in a model for the metabolites to assess total exposures to siloxanes, development of a pharmacokinetic/pharmacodynamic model to study concentration response data for protein induction, enzyme activity, and liver weight changes demonstrated that the hepatic responses following D_4 exposure are more likely to be related to parent D_4 than to metabolites (Sarangapani *et al.,* 2002). Additional evidence for the role of parent D_4 is from structural reasons in relation to other xenobiotics that have phenobarbital-like induction in liver (Waxman, 1999). Unfortunately there is no specific information available on the toxicity of the individual metabolites for comparison with the studies of parent D_4.

Blood:Air Partition Coefficient

The average value of Pb for humans estimated by fitting the model to the *in vivo* data was 0.96. The *in vitro* partition coefficient between rat blood and air was determined to be 4.3, while the Pb value required to describe the rat inhalation kinetics *in vivo* was also close to 1.0 (Andersen *et al.,* 2001). Several investigators have noted that Pb values for volatile compounds are usually larger by about a factor of two for rat blood compared to human blood (Gargas *et al.,* 1989). Thus, all available results are consistent with a Pb for D_4 in humans near unity.

Recently, Luu and Hutter (2001) developed a PBPK model for D_4 inhalation exposures in humans and rats that used a much different Pb, i.e., 20. The reasons for their use of a much larger Pb value were due to an oversight in the development of their rat model and the application of an unnatural constraint in the development of their human model (Andersen *et al.,* 2002). They used total radioactivity in blood from the rat inhalation study without differentiating parent D_4 from metabolites. Thus, their model fit the combined amount of D_4 and metabolite in blood as if it were parent D_4, even though by the end of the 6-h inhalation exposure in rats, the majority of radioactivity in blood was metabolite. Because of this oversight, a higher Pb value was required to maintain higher blood concentrations over time than due to D_4 alone. In their human model, they applied the higher Pb to the human data set of Utell *et al.* (1998). They then used the total amount absorbed during exposure, about 11% of the total inhaled, not as an outcome to be matched by the model, but as a physical constraint. With this unnatural constraint for a PBPK model with a volatile compound, a much higher Pb is required to retain all inhaled compound. Our PBPK model for D_4 was developed following the common approach for inhalation exposures to volatile compounds and describing D_4 plasma concentrations without artificial constraints on uptake. Because our model described Ca using Equation 2, the proportion retained was an output of the model and not a constraint.

Retention Efficiency

Recently, Csanady and Filser (2001) modeled the effects of Pb, QC, and QP on chemical uptake during inhalation exposures with varying workloads, noting that increased physical activity can increase uptake. The effect of exercise on absorption during inhalation exposures can be studied using Equation 2. For a short time early in an exposure when the concentration in the venous return is low (i.e., Cv $\sim$ 0), the proportion of absorbed chemical is as large as possible, and Equation 2 becomes

$$\frac{\text{Ca}}{\text{Cin}} = \frac{(\text{QP/QC})}{1 + (\text{QP/QC})/\text{Pb}}. \quad (6)$$

For chemicals with a high Pb, Ca/Cin would be approximately equal to QP/QC. The ratio QP/QC increases with exercise. For example, the ratio was experimentally determined to be about 0.8 at rest and about 2.0 at a workload of 50 W by Astrand (1983). Thus, exercise would increase the amount of chemical absorbed into the blood stream. However, for chemicals like D_4 with a low Pb, Ca/Cin will not be greatly affected by increasing QP/QC. A plot of Ca/Cin as a function of Pb, as predicted by Equation 6, shows that early in an exposure the effect of exercise on the ratio of Ca/Cin is minor for chemicals with Pb $<$ 1 (Fig. 11A). This result is consistent with Csanady and Filser, who concluded that for chemicals with a Pb $>$ 6, physical activity at work should be taken into account when determining occupational limit concentrations in air.

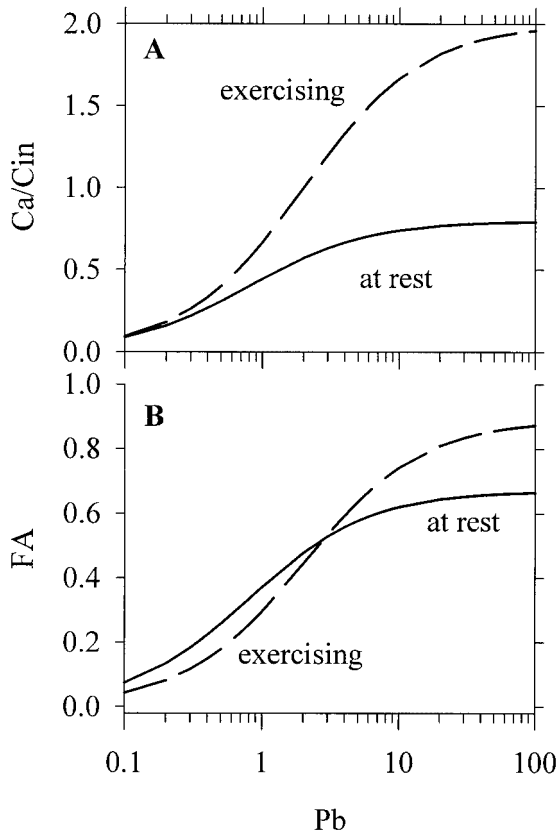

FIG. 11. The effect of exercise on (A) Ca/Cin (calculated using Equation 3) and (B) FA (calculated using Equation 5) as a function of Pb for short exposures where Cv $\sim$ 0. At rest, QP/QC = 0.8 and FDS = 0.33 (solid curve) and while exercising, QP/QC = 2.0 and FDS = 0.11 (dashed curve).

Exercise can also affect the fraction absorbed, FA (i.e., the fraction of chemical entering the lungs that absorbs into lung blood), defined as

$$\text{FA} = \frac{\text{Cin} - \text{Cex}}{\text{Cin}}. \quad (7)$$

To determine Cex, Calv (i.e., Ca/Pb) must be adjusted for the concentration of chemical in the dead space of the lungs as follows:

$$\text{Cex} = \text{FDS} \times \text{Cin} + (1 - \text{FDS}) \times \text{Calv} \quad (8)$$

where FDS is the fraction of dead space in the lungs, which also decreases with exercise. In the study of Astrand (1983), FDS was about 0.33 at rest and about 0.11 with a workload of 50 W. Equation 9, developed from Equations 6, 7, and 8, shows the effect of increasing QP/QC on FA:

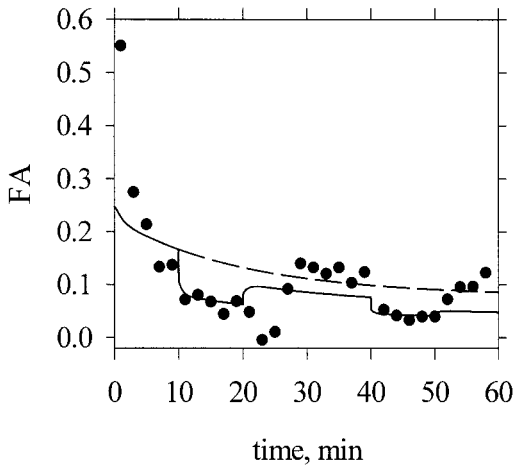

FIG. 12. Experimentally determined and simulated fraction absorbed (FA) as a function of time for Subject 1. The dashed curve was calculated assuming Subject 1 was at rest during the entire exposure while the solid curve was simulated including the physiological effects of periodic exercise in the PBPK model.

$$FA = \frac{1 - FDS}{1 + (QP/QC)/Pb}. \quad (9)$$

This equation predicts that FA will decrease during exercise for chemicals with $Pb < 3$, but increase during exercise for chemicals with $Pb > 3$ (Fig. 11B). FA also decreases as the length of the exposure increases because as tissue compartments fill, Cv increases and the rate of absorption of chemical from the lung air into the lung blood decreases. However, processes that result in chemical clearing from the bloodstream (e.g., metabolism) increase the rate of absorption during an inhalation exposure.

Utell *et al.* (1998) reported that during inhalation exposures to D_4, FA decreased with increased alveolar ventilation during exercise. Because the D_4 PBPK model included the major physiological effects of exercise, it quantitatively demonstrates how both exercise and time affect blood and exhaled D_4 concentrations. A simulation of FA as a function of time by the refined PBPK model for Subject 1 (Fig. 12) illustrates the changes in retention with different workloads and with increasing time. For the simulation where Subject 1 is exposed to 10 ppm ^{14}C-D_4 at rest, early in the exposure FA was about 0.25, but as tissues fill up and the venous blood concentration rises, FA decreased. The simulated curve is more complex when the effects of exercise are included. In general, FA decreased with time, but FA also periodically increased and then decreased as physiological properties changed. Consistent with our calculated value of $Pb = 0.96$, the decrease of FA with exercise indicates that Pb is below 3.0 (Fig. 11).

Summary

The human inhalation PBPK model for D_4 presented here described all available pharmacokinetic data for D_4 disposition in humans following inhalation exposures. D_4 has the unusual combination of low blood:air and high fat:blood partitioning, giving rise to preferential storage in lipid compartments in the body, including some sequestration in blood, and rapid elimination from all tissues other than fat after cessation of exposure. This PBPK model for D_4 provides a tool to quantify transport of highly lipophilic chemicals throughout the blood and tissues and to quantitatively characterize the retention, distribution, and elimination of parent D_4 and its hydrolysis and oxidation products from the body following inhalation exposures to humans. The human D_4 model is similar to the rat model, with similar partition coefficients and compartmental structures. The success in developing consistent PBPK models for D_4 in two species indicates that this human model should be useful for simulating tissue dosimetry of D_4 in humans exposed by inhalation and to further support the risk assessment of D_4.

APPENDIX 1

Simple Model

By modeling the lungs as a well-mixed compartment with an average, one-directional airflow in the region of gas exchange (i.e., QP), and with rapid equilibration between lung air and blood in the lung alveoli, the concentration in the blood exiting the lungs, Ca, can be described as

$$Ca = \frac{QP \times Cin + QC \times CBLV}{QC + QP/Pb} \quad (A\text{-}1)$$

where CBLV is the free concentration of D_4 in the venous blood compartment and Cin was 10 ppm D_4 during the exposure and zero after the exposure ended. The concentration of D_4 in exhaled breath, Cex, can be calculated using Equation 8, with Calv = Ca/Pb. Separate compartments were included for the venous and arterial blood. The mass balance for the concentration of D_4 in the arterial blood compartment, CBLA, is

$$VBLA \frac{dCBLA}{dt} = QC \times (Ca - CBLA) \quad (A\text{-}2)$$

where t is time and VBLA is the volume of the arterial blood compartment. The rate of mass transfer of D_4 into the fat, rapidly and slowly perfused tissues, and liver was limited by the blood flow to the tissues, as shown in A-3 to A-6:

$$VF \frac{dCF}{dt} = QF \times \left(CBLA - \frac{CF}{PF} \right) \quad (A\text{-}3)$$

$$VR \frac{dCR}{dt} = QR \times \left(CBLA - \frac{CR}{PR} \right) \quad (A\text{-}4)$$

$$VS \frac{dCS}{dt} = QS \times \left(CBLA - \frac{CS}{PS} \right) \quad (A\text{-}5)$$

$$VL \frac{dCL}{dt} = QL \times \left(CBLA - \frac{CL}{PL} \right) - KF \times \frac{CL}{PL} \quad (A\text{-}6)$$

where CF, CR, CS, and CL are the concentrations of D_4 in the fat, rapidly and slowly perfused tissues, and liver, respectively. Because D_4 is metabolized in the liver, A-6 includes the first-order clearance constant KF. The blood flows from the organ compartments combine in a mixed venous return compartment:

$$\text{VBLV}\frac{\text{dCBLV}}{\text{dt}} = \text{QF} \times \frac{\text{CF}}{\text{PF}} + \text{QL} \times \frac{\text{CL}}{\text{PL}} + \text{QR} \times \frac{\text{CR}}{\text{PR}} + \text{QS} \times \frac{\text{CS}}{\text{PS}} - \text{QC} \times \text{CBLV} \quad \text{(A-7)}$$

where VBLV is the volume of the venous blood compartment. A one-compartment model was used to describe the disposition of the pooled metabolites with first-order renal clearance as shown in A-8:

$$\text{VDIS}\frac{\text{dCMET}}{\text{dt}} = \text{KF} \times \frac{\text{CL}}{\text{PL}} - \text{KEL} \times \text{CMET} \quad \text{(A-8)}$$

where CMET and VDIS are the blood plasma concentration and volume of distribution of the combined metabolite pool, respectively. The amount of total metabolite excreted into urine, AMEX, can be calculated using the equation

$$\frac{\text{dAMEX}}{\text{dt}} = \text{KEL} \times \text{CMET}. \quad \text{(A-9)}$$

At the beginning of the exposure, the concentration of D_4 in all compartments was assumed to be zero (i.e., CA = 0, CBLA = 0, CF = 0, CR = 0, CS = 0, CL = 0, and CBLV = 0 at t = 0), and the concentration of metabolite in the blood plasma and the amount of metabolite in the urine were assumed to be zero (i.e., CMET = 0 and AMEX = 0 at t = 0).

Refined Model

The refined model has a mobile lipid pool in blood with D_4 that does not equilibrate with free D_4 in blood. This lipid pool is generated in the liver and cleared by the fat. The mass balance on the liver, A-6, then becomes

$$\text{VL}\frac{\text{dCL}}{\text{dt}} = \text{QL} \times \left(\text{CBLA} - \frac{\text{CL}}{\text{PL}}\right) - \text{KF} \times \frac{\text{CL}}{\text{PL}} - \text{Kmlp} \times \text{VL} \times \frac{\text{CL}}{\text{PL}}. \quad \text{(A-10)}$$

This sequestered D_4 in blood is cleared in the fat compartment, where D_4 can also move into a deep fat compartment, and so Equation A-3 becomes

$$\text{VF}\frac{\text{dCF}}{\text{dt}} = \text{QF} \times \left(\text{CBLA} - \frac{\text{CF}}{\text{PF}}\right) + \frac{\text{QF} \times \text{CLmlp}}{\text{QF} + \text{CLmlp}} \times \text{CAmlp} - \text{KFD} \times \text{CF} \times \text{VF} + \text{KDF} \times \text{AFD} \quad \text{(A-11)}$$

where CAmlp is the concentration of unavailable D_4 (i.e., in the mobile lipid pool) in the arterial blood and AFD is the amount of D_4 in the deep fat compartment, which is described as

$$\frac{\text{dAFD}}{\text{dt}} = \text{KFD} \times \text{CF} \times \text{VF} - \text{KDF} \times \text{AFD}. \quad \text{(A-12)}$$

The mass balances for unavailable D_4 in the arterial and venous blood are

$$\text{VBLA}\frac{\text{dCAmlp}}{\text{dt}} = \text{QC} \times (\text{CVmlp} - \text{CAmlp}) - \frac{\text{QF} \times \text{CLmlp}}{\text{QF} + \text{CLmlp}} \times \text{CAmlp} \quad \text{(A-13)}$$

$$\text{VBLV}\frac{\text{dCVmlp}}{\text{dt}} = \text{Kmlp} \times \text{VL} \times \frac{\text{CL}}{\text{PL}} - \text{QC} \times (\text{CVmlp} - \text{CAmlp}) \quad \text{(A-14)}$$

where CVmlp is the concentration of unavailable D_4 (i.e., in the mobile lipid pool) in the venous blood. The average concentration of total D_4 (i.e., free and bound) in the mixed venous return, CVMIX, can be calculated as

$$\text{CVMIX} = \text{CBLV} + \text{CVmlp}. \quad \text{(A-15)}$$

At the beginning of the exposure, the concentration of unavailable D_4 in both the arterial blood and venous blood is assumed to be zero (i.e., CAmlp = 0 and CVmlp = 0 at t = 0).

In the refined model, the mass transfer in the slowly perfused compartment was limited by diffusion into the tissue. The mass balance on the slowly perfused compartment becomes

$$\text{VS}\frac{\text{dCS}}{\text{dt}} = \text{PAS} \times \left(\text{CBLA} - \frac{\text{CS}}{\text{PS}}\right). \quad \text{(A-16)}$$

In this case, the blood exiting the slowly perfused tissue compartment has not equilibrated with the compartment (i.e., the concentration in blood plasma leaving the slowly perfused compartment, CVS, is not equal to CS/PS), as illustrated by A-17:

$$\text{CVS} = \text{CBLA} - \frac{\text{PAS}}{\text{QS}} \times \left(\text{CBLA} - \frac{\text{CS}}{\text{PS}}\right). \quad \text{(A-17)}$$

Finally, the mass balance equation for the venous return becomes

$$\text{VBLV}\frac{\text{dCBLV}}{\text{dt}} = \text{QF} \times \frac{\text{CF}}{\text{PF}} + \text{QL} \times \frac{\text{CL}}{\text{PL}} + \text{QR} \times \frac{\text{CR}}{\text{PR}} + \text{QS} \times \text{CVS} - \text{QC} \times \text{CBLV}. \quad \text{(A-18)}$$

For the refined model, A-18 replaces A-7.

A model describing the plasma concentration of metabolites tetramer-triol, trimer-diol, dimer-diol, monomer-diol, and monomer-triol (i.e., CIVT, CIIID, CIID, CID, and CIT, respectively) was also developed. Instead of including a one-compartment model for a combined metabolite pool, a one-compartment model was included for each individual metabolite. The volume of distribution for each metabolite was assumed to be the same as it was for the combined metabolite pool. The rate of change of the metabolite concentrations are described as follows:

$$\text{VDIS}\frac{\text{dCIVT}}{\text{dt}} = \text{KF} \times \frac{\text{CL}}{\text{PL}} - \text{K1} \times \text{CIVT} \quad \text{(A-19)}$$

$$\text{VDIS}\frac{\text{dCIIID}}{\text{dt}} = \text{K1} \times \text{CIVT} - (\text{K2} + \text{KEL4}) \times \text{CIII}D \quad \text{(A-20)}$$

$$\text{VDIS}\frac{\text{dCIID}}{\text{dt}} = \text{K2} \times \text{CIIID} - (\text{K3} + \text{KEL3}) \times \text{CIID} \quad \text{(A-21)}$$

$$\text{VDIS}\frac{\text{dCID}}{\text{dt}} = \text{K2} \times \text{CIIID} + 2 \times \text{K3} \times \text{CIID} - (\text{K4} + \text{KEL2}) \times \text{CID} \quad \text{(A-22)}$$

$$\text{VDIS}\frac{\text{dCIT}}{\text{dt}} = \text{K1} \times \text{CIVT} + \text{K4} \times \text{CID} - \text{KEL1} \times \text{CIT} \quad \text{(A-23)}$$

where K1, K2, K3, and K4 are first-order reaction rate constants for the metabolism of tetramer-triol, trimer-diol, dimer-diol, and monomer-diol, respectively, as shown in Figures 3 and 4. The cumulative amount of monomer-triol, monomer-diol, dimer-diol, and trimer-diol in the urine (i.e., AIT, AID, AIID, and AIIID, respectively) can be calculated using the equations:

$$\frac{dAIT}{dt} = KEL1 \times CIT \quad \text{(A-24)}$$

$$\frac{dAID}{dt} = KEL2 \times CID \quad \text{(A-25)}$$

$$\frac{dAIID}{dt} = KEL3 \times CIID \quad \text{(A-26)}$$

$$\frac{dAIIID}{dt} = KEL4 \times CIIID. \quad \text{(A-27)}$$

At the beginning of an exposure, the concentrations of all metabolites in blood plasma and the amount of all metabolites in the urine are assumed to be zero (i.e., CIVT = 0, CIIID = 0, CIID = 0, CID = 0, CIT = 0, AIT = 0, AID = 0, AIID = 0, and AIIID = 0 at t = 0).

APPENDIX 2

Notation

AFD, amount of D_4 in the deep fat compartment
AID, amount of monomer-diol in the urine
AIID, amount of dimer-diol in the urine
AIIID, amount of trimer-diol in the urine
AIT, amount of monomer-triol in the urine
BW, body weight
Ca, concentration of D_4 in the arterial blood exiting the lungs
Calv, concentration of D_4 in alveolar air
CAmlp, concentration of unavailable D_4 in the arterial blood
CBLA, concentration of D_4 in the arterial blood compartment
CBLV, concentration of D_4 in the venous blood compartment
Cex, concentration of D_4 in exhaled breath
CF, concentration of D_4 in the fat
CID, concentration of monomer-diol in the blood plasma
CIID, concentration of dimer-diol in the blood plasma
CIIID, concentration of trimer-diol in the blood plasma
Cin, inhaled concentration of D_4
CIT, concentration of monomer-triol in the blood plasma
CIVT, concentration of tetramer-triol in the blood plasma
CL, concentration of D_4 in the liver
CLex, clearance of D_4 by exhalation
CLmlp, clearance of unavailable D_4 from the blood into the fat
CMET, concentration of combined metabolite pool in blood plasma
CR, concentration of D_4 in the rapidly perfused tissue compartment
CS, concentration of D_4 in the slowly perfused tissue compartment
Cv, concentration of chemical in the venous return
CVMIX, concentration of total D_4 (i.e., available and unavailable) in the venous return
CVS, concentration of D_4 in the plasma exiting the slowly perfused tissue compartment when there is a diffusional resistance to mass transport in that compartment
CVmlp, concentration of unavailable D_4 in the venous blood
FDS, fraction of the lung volume where gas exchange does not occur (i.e., dead space)
K1, first-order reaction rate constant for the metabolism of tetramer-triol
K1C, allometric constant for calculating K1
K2, first-order reaction rate constant for metabolism of trimer-diol
K2C, allometric constant for calculating K2
K3, first-order reaction rate constant for the metabolism of dimer-diol
K3C, allometric constant for calculating K3
K4, first-order reaction rate constant for oxidation of monomer-diol
K4C, allometric constant for calculating K4
KDF, first-order mass transfer coefficient for the movement of D_4 from a deep compartment into the fat compartment
KEL, first-order rate of renal clearance for combined metabolite pool
KEL1, first-order rate constant for elimination of monomer-triol from plasma into urine
KEL2, first-order rate constant for elimination of monomer-diol from plasma into urine
KEL3, first-order rate constant for elimination of dimer-diol from plasma into urine
KEL4, first-order rate constant for elimination of trimer-diol from plasma into urine
KF, first-order clearance constant for D_4 metabolism in the liver
KFC, allometric constant for calculating KF
KFD, first-order mass transfer coefficient for the movement of D_4 from the fat compartment into a deep compartment
Kmlp, first-order rate constant for production of mobile lipid pool in the liver
$K_{o/w}$, octanol/water partition coefficient
LSP, log-normalized sensitivity parameter
PAS, mass transfer coefficient for the slowly perfused tissue compartment
Pb, partition coefficient of D_4 between blood plasma and lung air
PF, partition coefficient of D_4 between fat and blood plasma
PL, partition coefficient of D_4 between liver and blood plasma
PR, partition coefficient of D_4 between rapidly perfused tissue and blood plasma
PS, partition coefficient of D_4 between slowly perfused tissue and blood plasma
QC, cardiac output
QF, blood flow rate to fat tissue
QL, blood flow rate to liver
QP, alveolar ventilation rate
QR, blood flow rate to rapidly perfused tissue
QS, blood flow rate to slowly perfused tissue
t, time
VBLA, volume of arterial blood compartment
VBLV, volume of venous blood compartment
VDIS, volume of distribution for the combined metabolite pool
VDISC, fraction of BW in the volume of distribution for the combined metabolite pool
VF, volume of fat compartment
VL, volume of liver compartment
VR, volume of rapidly perfused tissue compartment
VS, volume of slowly perfused tissue compartment

ACKNOWLEDGMENTS

This work was supported in part by the Silicones Environmental, Health and Safety Council of North America. We thank our colleagues at the Center for Environmental Toxicology and Technology, and especially R. Yang, for valuable discussions and encouragement. The efforts of D. Chalupa in performing the clinical inhalation studies and B. Gelein in developing and performing the analytical studies are appreciated. M.B.R. received support from grants numbers T32 ES07321 and F32 ES11425 from the National Institute of Environmental Health Sciences, NIH.

REFERENCES

Andersen, M. E, Sarangapani, R., Dobrev, I. D., Reitz, R. H., Plotzke, K. P., and Reddy, M. B. (2002). Letter to the Editor: Further comments on the bioavailability of D_4. *Environ. Health Perspect.* **110,** A444–A445.

Andersen, M. E., Sarangapani, R., Reitz, R. H., Gallavan, R. H., Dobrev, I. D., and Plotzke, K. P. (2001). Physiological modeling reveals novel pharmaco-

kinetic behavior for inhaled octamethylcyclotetrasiloxane in rats. *Toxicol. Sci.* **60,** 214–231.

Astrand, I. (1983). Effect of physical exercise on uptake, distribution, and elimination of vapors in man. In *Modeling of Inhalation Exposures to Vapors: Uptake, Distribution and Elimination,* Vol. II (V. Fiserova-Bergerova, Ed.), pp.107–130. CRC Press, Boca Raton, FL.

Brown, R. P., Delp, M. D., Lindstedt, S. L., Rhomberg, L. R., and Beliles, R. P. (1997). Physiological parameter values for physiologically based pharmacokinetic models. *Toxicol. Ind. Health* **13,** 407–484.

Bulow, J., and Madsen, J. (1978). Human adipose tissue blood flow during prolonged exercise II. *Pflugers Arch.* **376,** 41–45.

Clewell, H. J., III, Lee, T., and Carpenter, R. L. (1994). Sensitivity of physiologically based pharmacokinetic models to variation in model parameters: Methylene chloride. *Risk Anal.* **14,** 521–531.

Csanady, G. A., and Filser, J. G. (2001). The relevance of physical activity for the kinetics of inhaled gaseous substances. *Arch. Toxicol.* **74,** 663–672.

Gargas, M. L., Burgess, R. J., Voisard, D. E., Cason, G. H., and Andersen, M. E. (1989). Partition coefficients of low-molecular-weight volatile chemicals in various liquids and tissues. *Toxicol. Appl. Pharmacol.* **98,** 87–99.

Jonsson, F., Bois, F., and Johanson, G. (2001). Physiologically based pharmacokinetic modeling of inhalation exposure of humans to dichloromethane during moderate to heavy exercise. *Toxicol. Sci.* **59,** 209–218.

Luu, H. M. D., and Hutter, J. C. (2001). Bioavailability of octamethylcyclotetrasiloxane (D_4) after exposure to silicones by inhalation and implantation. *Environ. Health Perspect.* **109,** 1095–1101.

McKim, J. M., Kolesar, G. B., Jean, P. A., Meeker, L. S., Wilga, P. C., Schoonhoven, R., Swenberg, J. A., Goodman, J. I., Gallavan, R. H., and Meeks, R. G. (2001). Repeated inhalation exposure to octamethylcyclotetrasiloxane produces hepatomegaly, transient hepatic hyperplasia, and sustained hypertrophy in female Fischer 344 rats in a manner similar to phenobarbital. *Toxicol. Appl. Pharmacol.* **172,** 83–92.

McKim, J. M., Wilga, P. C., Kolesar, G. B., Choudhuri, S., Madan, A., Dochterman, L. W., Breen, J. G., Parkinson, A., Mast, R. W., and Meeks, R. G. (1998). Evaluation of octamethylcyclotetrasiloxane (D_4) as an inducer of rat hepatic microsomal cytochrome P450, UDP-glucuronosyltransferase, and epoxide hydrolase: A 28-day inhalation study. *Toxicol. Sci*. **41,** 29–41.

MGA Software (1997). *ACSL Optimize User's Guide for Windows.* Concord, MA.

Plotzke, K. P., Crofoot, S. D., Ferdinandi, E. S., Beattie, J. G., Reitz, R. H., McNett, D. A., and Meeks, R. G. (2000). Disposition of radioactivity in Fischer 344 rats after single and multiple inhalation exposure to [^{14}C]octamethylcyclotetrasiloxane ($^{14}CD_4$). *Drug Metab. Dispos.* **28,** 192–204.

Ramsey, J. C., and Andersen, M. E. (1984). A physiologically based description of the inhalation pharmacokinetics of styrene in rats and humans. *Toxicol. Appl. Pharmacol.* **73,** 159–175.

Salyers, K. L., Varaprath, S., McKim, J. M., Jr., Mast, R. W., and Plotzke, K. P. (1996). Disposition and metabolism of octamethylcyclotetrasiloxane (D_4) in F-344 rats: Effect of classical inducing agents. *Toxicologist* **30,** 15 (Abstract).

Sarangapani, R., Teeguarden, J., Plotzke, K. P., McKim, J. E., Jr., and Andersen, M. E. (2002). Dose-response modeling of Cytochrome P450 induction in rats by octamethylcyclotetrasiloxane. *Toxicol. Sci.* **67,** 159–172.

Utell, M. J. (2000). Absorption, kinetics and elimination of ^{14}C-octamethylcyclotetrasiloxane (C-14 D_4) in humans after a one h respiratory exposure. Report to the Dow Corning Corporation.

Utell, M. J., Gelein, R., Yu, C. P., Kenaga, C., Geigel, E., Torres, A., Chalupa, D., Gibb, F. R., Speers, D. M., Mast, R. W., and Morrow, P. E. (1998). Quantitative exposure of humans to an octamethylcyclotetrasiloxane (D_4) vapor. *Toxicol. Sci.* **44,** 206–213.

Varaprath, S., Salyers, K. L., Plotzke, K. P., and Nanavati, S. (1999). Identification of metabolites of octamethylcyclotetrasiloxane (D_4) in rat urine. *Drug Metab. Dispos.* **27,** 1267–1273.

Varaprath, S., Seaton, M., McNett, D. A., Cao, L., and Plotzke, K. P. (2000) Quantitative determination of octamethycyclotetrasiloxane (D_4) in extracts of biological matrices by gas chromatography-mass spectrometry. *Intern. J. Environ. Anal. Chem.* **77,** 203–219.

Waxman, D. J. (1999). P450 gene induction by structurally diverse xenochemicals: Central role of nuclear receptors CAR, PXR, and PPAR. *Arch. Biochem. Biophys.* **369**, 11–23.

Zhang, J., Falany, J. L., Xie, X., and Falany, C. N. (2000). Induction of rat hepatic drug metabolizing enzymes by dimethylcyclosiloxane. *Chem. Biol. Interact.* **124,** 133–147.